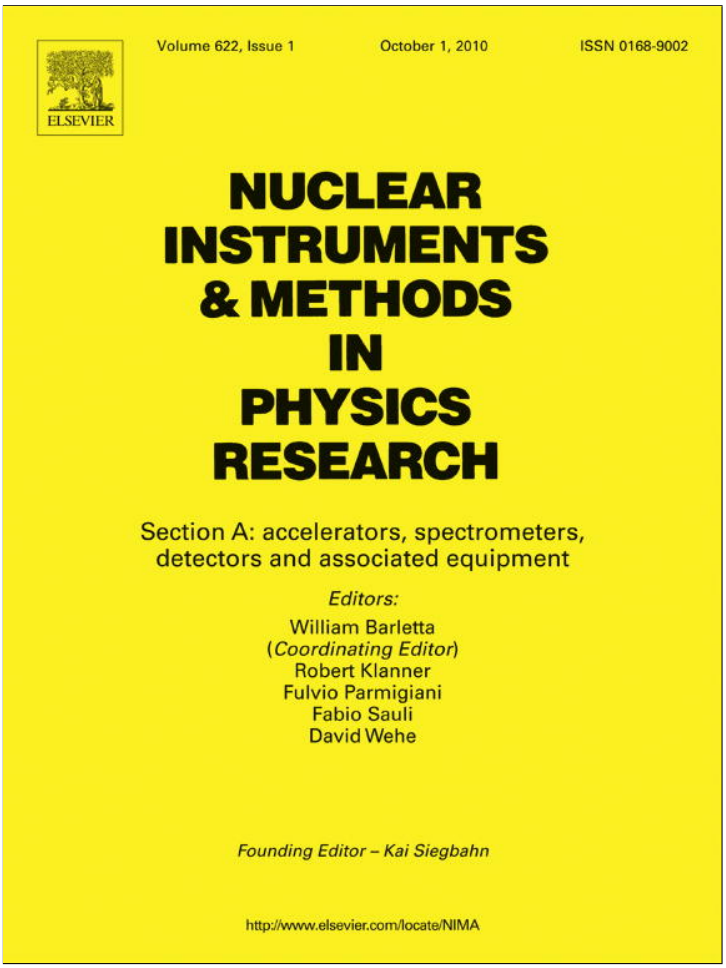

Nuclear Instruments and Methods in Physics Research A 622 (2010) 191–195

Contents lists available at ScienceDirect

Nuclear Instruments and Methods in Physics Research A

journal homepage: www.elsevier.com/locate/nima

Neutron spectroscopy of plutonium oxide using matrix unfolding approach

Tomasz Zak [a], Shaun D. Clarke [a,*], Mark M. Bourne [a], Sara A. Pozzi [a], Yunlin Xu [a], Thomas J. Downar [a], Paolo Peerani [b]

[a] University of Michigan, Department of Nuclear Engineering and Radiological Sciences, 2328B Cooley Building, 2355 Bonisteel Blvd. Ann Arbor, MI 48109, USA
[b] European Commission EC-JRC-IPSC, Ispra, Italy

ARTICLE INFO

Article history:
Received 12 March 2010
Received in revised form
29 June 2010
Accepted 2 July 2010
Available online 15 July 2010

Keywords:
Plutonium oxide
Neutron spectroscopy
Detector response matrix

ABSTRACT

The knowledge of a neutron energy spectrum is extremely valuable in nuclear non-proliferation and safeguards applications. Unfortunately, conventional gas and fission-type detectors are not adapted to determine incident neutron energy. As a result, a matrix inversion technique was implemented to generate desirable and consistent neutron energy spectra from an EJ-309 liquid scintillator. To overcome the ill-posed unfolded solutions, the method of sequential least squares is reviewed briefly, and the conditions under which it is used are stated. From the analysis, unfolded energy spectra solutions of five distinct PuO_2 fuel samples and a ^{252}Cf source are presented and compared to the simulated unfolded and reference energy distributions.

1. Introduction

The physical properties of liquid scintillators make them ideal for the measurement of fast neutrons. Liquid scintillators provide good efficiency for neutron interactions by elastic scattering collisions. Spectral averaged efficiencies vary, but are typically around 30–70%, depending on the size of the liquid cell [1]. These properties, plus the ability to discriminate neutrons from gamma rays, make liquid scintillators an excellent choice for nuclear non-proliferation and safeguards applications [2].

The knowledge of the neutron energy spectrum is extremely valuable in many applications. The energy spectrum of neutron sources for various applications varies greatly. For example, (α, n) sources used in medical or oil-well-logging applications has a very different energy spectrum that fission sources from special nuclear material (or ^{252}Cf). Unfortunately, commonly used neutron detectors, such as an He-3 proportional tubes, Bonner spheres, and BF_3 tubes require moderation and cannot be used to determine incident neutron energy with reasonable efficiency. As a result, a response matrix inversion algorithm was implemented to generate consistent unfolded neutron energy spectra from an EJ-309 liquid scintillator. The ill-posed problem is optimized through a sequential least squares method (SLSM).

In a recent experiment [3], pulse-height-distributions (PHDs) of five PuO_2 samples and a ^{252}Cf source were measured. In this paper, these PHDs are simulated using MCNP-PoliMi and both simulated and measured PHDs are unfolded using the SLSM. The results of both the measured and simulated data unfolding will be compared to the reference neutron energy distributions.

2. Spectrum unfolding methods

2.1. Sequential least squares approach

The pulse-height distribution measured with a scintillation detector includes information on the energy spectrum of the incident neutrons. The relationship between the pulse height distribution and the energy spectrum is uniquely characterized by the detector "response matrix". However, uncovering this relationship is difficult because the unfolding problem is ill-posed [4–6]. Previous attempts have shown that practical unfolded results can be obtained with an applied sequential least squares method [7]. In order to improve upon this method, the algorithm was made more versatile: now accepting a user-defined detector response matrix of any size.

The detector response, incident neutron flux, and the neutron count rate are all related through the Fredholm integral of the first kind given by

$$N(L) = \int R(E_n,L)\Phi(E_n)\,dE_n \tag{1}$$

where E_n is the neutron energy, L is the measured light output, $N(L)$ is the count rate density, and $R(E_n, L)$ is the detector response matrix. The problem can be solved by discretizing the above

* Corresponding author. Tel.: +1 734 615 7830; fax: +1 734 763 4540.
E-mail address: clarkesd@umich.edu (S.D. Clarke).

0168-9002/$ - see front matter © 2010 Elsevier B.V. All rights reserved.
doi:10.1016/j.nima.2010.07.029

integral to its constituent components given by

$$N_i = \sum_{j=1}^{m} R_{ij} x_j, \quad \text{for } i = 1,..,n, \tag{2}$$

where N_i is the flux count rate corresponding to a certain interval of the measured light output in the i-th channel, x_j is the incident neutron fluence in the j-th energy group, and R_{ij} is the corresponding element of the response matrix.

If the number of pulse height bins is the same as the number of neutron energy groups in the response matrix R, then the neutron spectrum can be obtained by solving the linear system by a matrix inversion

$$x = R^{-1} N \tag{3}$$

If the number of light output channels is greater than the number of neutron energy groups in the response matrix, then the system becomes over-determined and can be solved by a least squares method.

Inherent statistical errors exist in both the response matrix R, and in the detector response N. Because the problem is so ill-posed, these errors contribute significantly to the solution and may result in negative fluxes when the least squares approach is applied. Consequently, a constrained optimization method is implemented to achieve physical unfolded solutions. The optimization problem is defined as

$$\min f(x) = \frac{1}{2} \sum_{i=1}^{n} w_i \left(N_i - \sum_{j=1}^{m} R_{ij} x_j \right)^2$$
$$x_i \geq 0 \quad \text{for } i \in S_B \equiv \{1,2,...,m\} \tag{4}$$

S_B refers to the set of indices for the lower bounds, which ensures that fluxes remain non-negative.

2.2. Detector response matrix

A response matrix was generated and used as an input to the unfolding algorithm. The matrix was constructed by tracking particle histories, using the simulation code MCNP-PoliMi [8]. Previous work has shown that an MCNP-PoliMi can be used to accurately calculate the detector response matrix [9].

The EJ-309 liquid scintillator that was used in the measurements was simulated using an MCNP-PoliMi. Monoenergetic neutrons were simulated to produce a matrix response of scintillation light output as a function of an incident neutron energy. The final response matrix was constructed with a dimensional resolution of 201 light output bins (0.05-MeVee bin width) and 150 neutron energy bins (0.1-MeV bin width). The final response matrix is illustrated in Fig. 1. Each row corresponds to a single incident neutron energy and each column corresponds to the possible light output intensities for each neutron collision. As expected, higher energy neutrons can produce larger light output values. The ridge with higher intensities is formed from neutron scattering on carbon nuclei in the scintillation liquid. Carbon produces smaller light outputs per scintillation.

2.3. Energy group collapsing

The unfolding algorithm is capable of collapsing adjacent neutron energy groups within the response matrix to produce an averaged energy group of larger energy bin width. The unfolding script utilizes an interpolation technique that uses a moving average to correct the energy spacing in the original input pulse height distribution. This interpolation technique reduces the statistical oscillations in the higher energy region of the PHD. This procedure decreases the total amount of obtainable unfolded data points, but generally provides a more stable unfolded solution.

3. Measurement techniques

3.1. Fissile material

Measurements were performed at the JRC-Ispra, Italy on five PuO_2 samples stored in cylindrical steel containers with various heights and diameters. The canisters contained between 50 and 500 g of either high- or low-burnup PuO_2. A 2500 neutrons per second certified ^{252}Cf source was also used in a separate measurement. Table 1 summarizes the burnup and mass of each

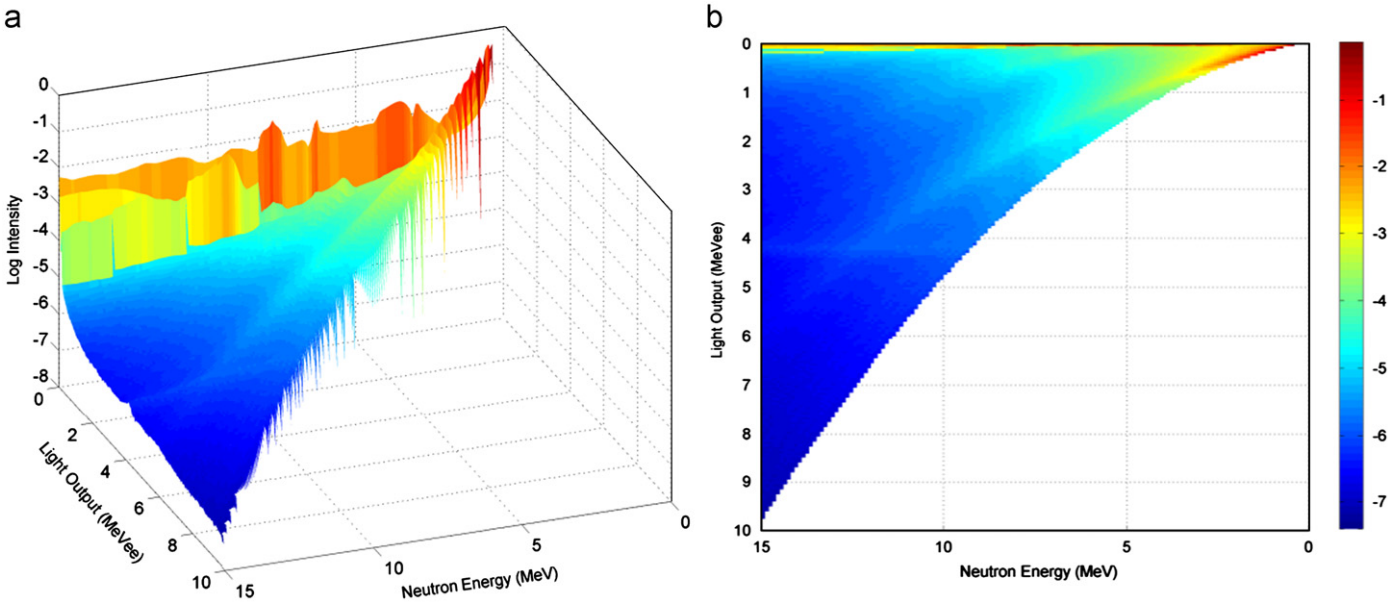

Fig. 1. Simulated EJ-309 detector response matrix: the three dimensional matrix is shown in (a) and the two-dimensional projection is shown in (b). Each neutron energy bin corresponds to an entire column of possible light output pulse height values. The dimensions of the matrix are 150 neutron energy bins and 201 light output bins.

Table 1
Sample composition and burnup.

Sample	Net mass (g)	^{238}Pu (wt%)	^{239}Pu (wt%)	^{240}Pu (wt%)	^{241}Pu (wt%)	^{242}Pu (wt%)	Burnup
103	49.595	1.72	58.10	24.77	9.77	5.65	High
104	98.089	0.20	70.96	24.58	3.29	0.98	Low
106	100.456	1.72	58.10	24.77	9.77	5.65	High
107	298.089	0.20	70.96	24.58	3.29	0.98	Low
109	501.984	0.20	70.96	24.58	3.29	0.98	Low

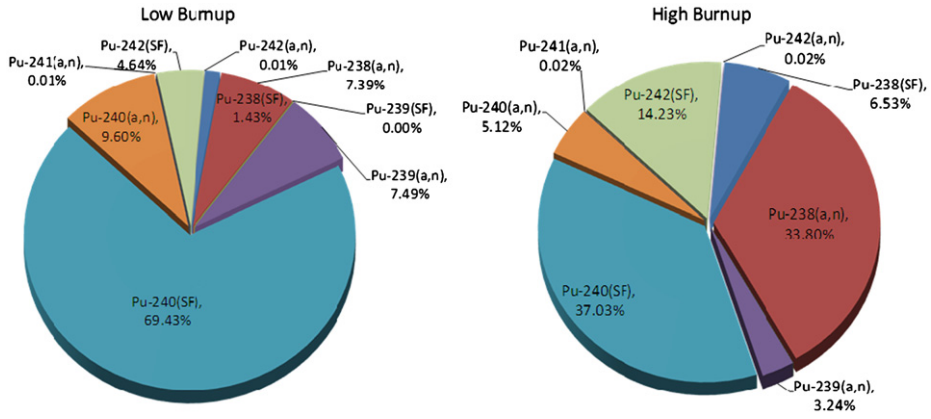

Fig. 2. Fraction of spontaneous fission (*s.f.*) and (α, n) neutrons emitted from low- and high-burnup PuO_2 samples. ^{239}Pu(*s.f.*), ^{241}Pu(*s.f.*), ^{241}Pu(α, n), and ^{241}Pu(α, n) reactions were negligible because of low (less than 0.01%) intensities.

PuO_2 sample [10]. Furthermore, Fig. 2 displays the fraction of total neutrons produced in the high- and low-burnup samples.

In the case of the high burnup samples (samples 103 and 106), the (α, n) contribution is more significant than that of the low burnup samples (samples 104, 107, and 109). This effect results from the higher ^{238}Pu and ^{240}Pu content from longer irradiation times. The alpha reaction on oxygen produces a continuous neutron emission spectrum that has a significant peak at 2.3 MeV [11]. This peak is present in all samples, but is especially prevalent in the high burnup samples. Although the (α, n) spectrum is harder than the spontaneous fission spectrum, the fission spectrum is more dominant at energies greater than 3 MeV.

3.2. Measurement technique

The measurement setup consisted of six EJ-309 liquid scintillation detectors (13.3 cm high and 13 cm in diameter) with Photonis XP4512B photomultiplier tubes (PMTs). The detectors were all positioned symmetrically around the sample at distance of 30 cm. Lead shielding sleeves of approximately 2.6 cm in thickness were placed around the sample to minimize the gamma ray background intensity. A detailed description of the experimental setup and procedure can be found in [12].

A CAEN V1720, 12-bit, 250-MHZ digitizer was used to sample and store signal pulses directly from the detector. A detection threshold of 100-keVee (corresponding to a deposited neutron energy of approximately 600 keV) was applied to the detector. The data acquisition time was less than 5 min per sample. The counts in the four axial detectors were averaged to generate the distributions shown in the following analysis.

3.3. Pulse height distributions

Measured neutron pulse height distributions for each of the PuO_2 samples and the ^{252}Cf source were obtained through the CAEN digitizer and an offline pulse shape discrimination technique was used to distinguish gamma and neutron events [13].

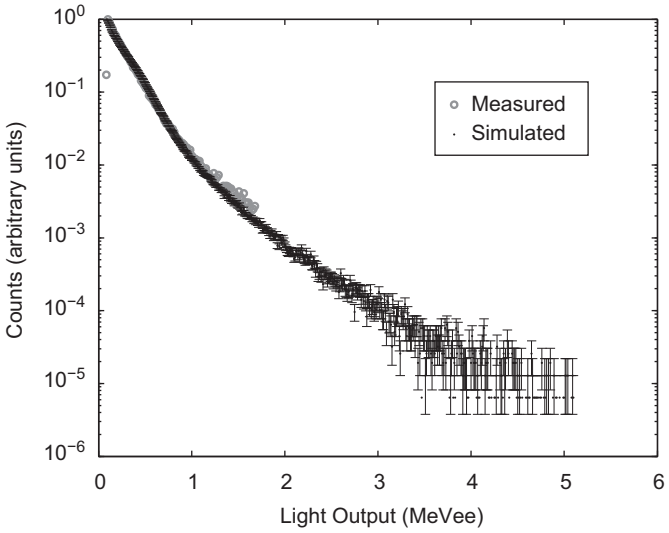

Fig. 3. Simulated and measured neutron PHDs for sample 109 ($1-\sigma$ statistical error bars are shown on the simulated results).

Simulated neutron pulse height distributions were created with the MCNP-PoliMi code. The simulated setup consisted of a detailed sample canister with the PuO_2 surrounded by the lead sleeve. For simplicity the detectors were modeled as purely active volumes.

The collision information from the MCNP-PoliMi output data file was post-processed with a specifically designed FORTRAN algorithm. The algorithm produces a neutron pulse height distribution based on various physical parameters of the scintillator detector. Such parameters include the light conversion

efficiency and basic material characteristics of the scintillation liquid.

Two pulse height distributions from sample 109 are shown in Fig. 3. The simulated and measured are normalized to their integrals. The simulated-PHD obtained relatively good statistics even light outputs greater than 3 MeVee. On the other hand, the 2-V dynamic range of the CAEN digitizer limited the maximum obtainable light output of the measured sample to approximately 1.7 MeVee.

4. Spectrum unfolding results

4.1. Unfolded results

The resulting unfolded neutron energy spectra for ^{252}Cf and the five PuO_2 samples are shown in Figs. 4–9. Both measured and simulated unfolded energy spectra were compared to the reference energy spectrum (obtained from MCNP-PoliMi) of each

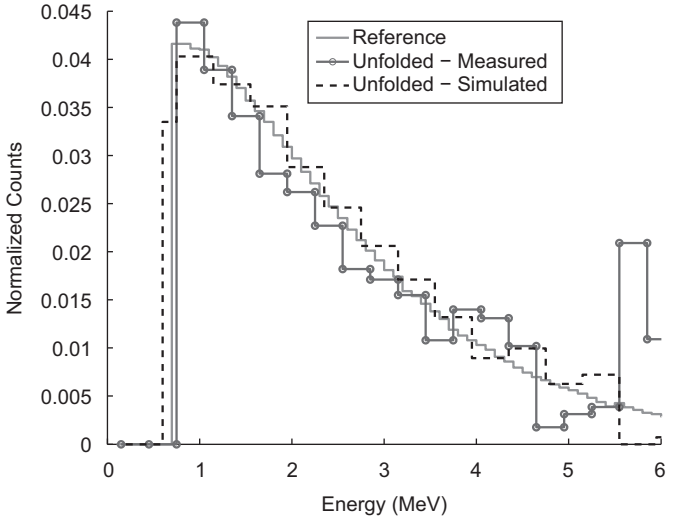

Fig. 4. Unfolded energy spectra from the measured and simulated PHDs compared to the reference energy spectrum of ^{252}Cf.

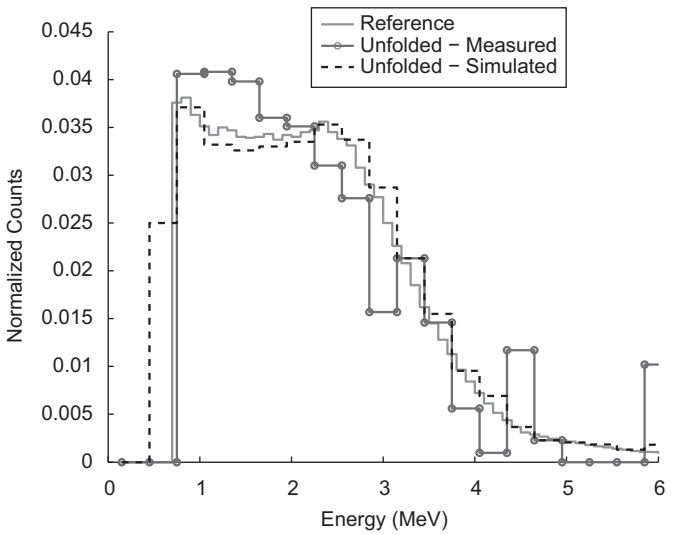

Fig. 5. Unfolded energy spectra from the measured and simulated PHDs compared to the reference energy spectrum of the 50 g high burnup PuO_2 sample (103).

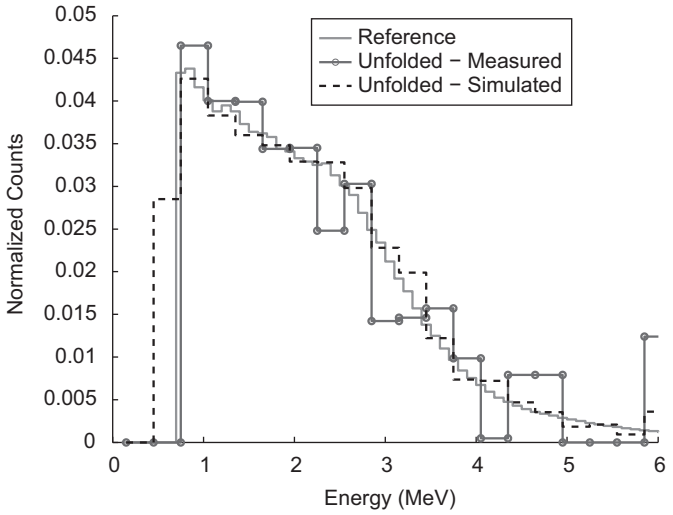

Fig.6. Unfolded energy spectra from the measured and simulated PHDs compared to the reference energy spectrum of the 100 g low burnup PuO_2 sample (104).

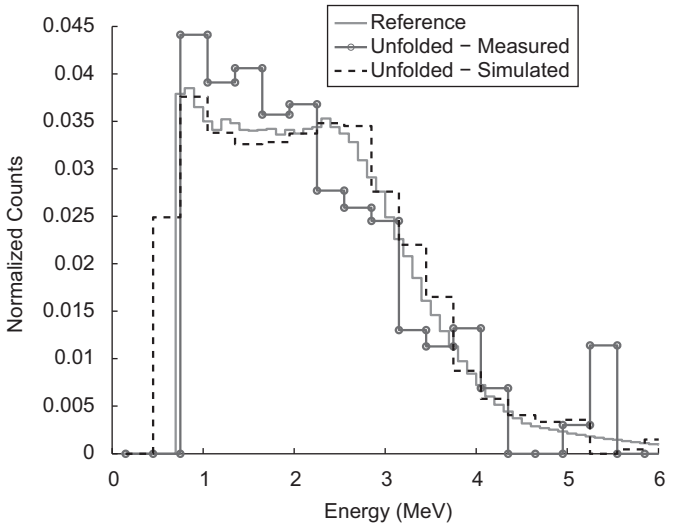

Fig. 7. Unfolded energy spectra from the measured and simulated PHDs compared to the reference energy spectrum of the 100 g high burnup PuO_2 sample (106).

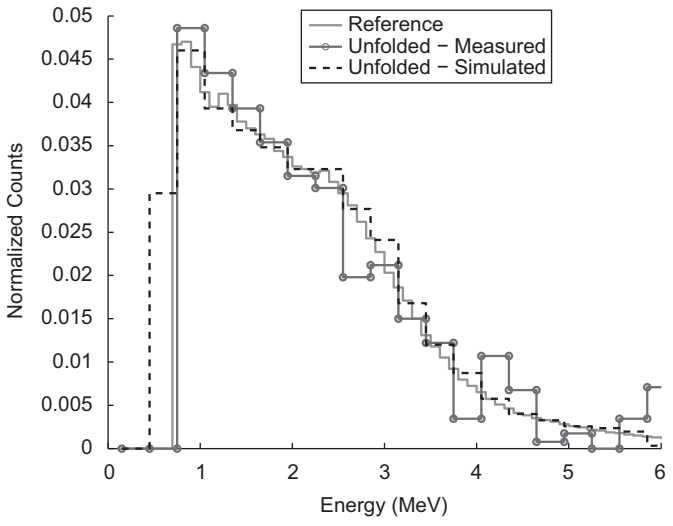

Fig. 8. Unfolded energy spectra from the measured and simulated PHDs compared to the reference energy spectrum of the 300 g low burnup PuO_2 sample (107).

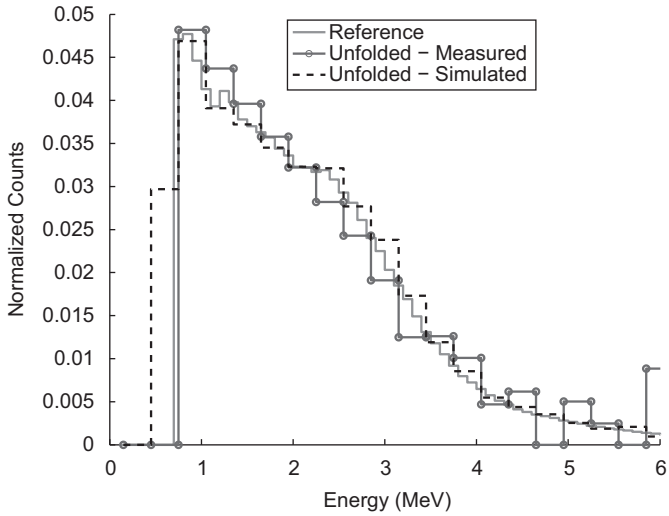

Fig. 9. Unfolded energy spectra from the measured and simulated PHDs compared to the reference energy spectrum of the 500 g low burnup PuO_2 sample (109).

sample. The measured, simulated, and reference were all normalized to their integral.

The results obtained were all obtained by collapsing three adjacent neutron bins in the matrix. This improved the behavior of the unfolded spectra, but decreased the maximum obtainable energy resolution to 300 keV. Measurements of the PuO_2 samples were limited to a lower threshold bound of 100 keVee, which corresponds to approximately 600 keV. Figs. 4–9 show these results for all samples.

4.2. Simulated-PHD unfolding analysis

The unfolded spectra obtained from the simulated PHDs show a very good fit to the reference spectra for all cases. Both the fission peak (approximately 0.8 MeV) and the (α, n) peak (approximately 2.3 MeV) were very well defined. The simulated PHDs provided enough data at large enough light outputs to allow reliable unfolding over the entire energy range. The input pulse height distribution had a detection threshold of 100 keVee, which corresponds to approximately 600-keV neutron energy deposited. Consequently, the first alpha peak at 400 keV cannot be characterized because it is below the detection threshold. The response matrix had a minimum energy of 250 keV, resulting in zero unfolded counts below this value. Tail response was also stable, although large statistical variations in the region greater than 2 MeVee (shown in Fig. 3).

4.3. Measured-PHD unfolding analysis

The measured data was obtained with a maximum recordable light output of 1.7 MeVee (because of the 2-V dynamic range of the digitizer). This corresponds to approximately 5.5 MeV neutron energy deposited. Consequently, neutrons depositing energy greater than this are not recorded. This results in a truncated PHD range and consequently a noisier unfolded energy spectrum. Decreasing the PMT gain in the measurement or using a digitizer with a larger dynamic range would mitigate these issues.

4.4. Error analysis

The inversion of the response matrix R is nontrivial. The matrix is not square and as a result the inversion problem is ill-conditioned. Statistical uncertainties in the response matrix $R(E, L)$ or pulse height distribution $N(L)$ from measured and simulated samples combine to give a numerically unstable solution. As a result, small changes in either the response matrix or pulse height distribution give rise to large variations in the unfolded flux. This problem is minimized by implementing a sequential least squares technique, where a first-guess solution for the unfolded spectrum is modified by repeated forward calculations of the response matrix and unfolded flux. This produces an estimate of the pulse height distribution which is iteratively updated. The statistical uncertainty in the unfolded solution is a function of the uncertainties in the detector response matrix and the measured-PHD. Efforts are underway to quantify the propagation of these errors through the unfolding process.

Also, large statistical variations were observed in all measured PHDs above 1 MeVee; increasing the counting time of the measurement could mitigate this effect. Furthermore, these ill-behaved oscillations in the PHD are interpolated through a moving average technique within the unfolding script to produce a more physical unfolded energy spectrum.

5. Conclusion

Unfolding neutron spectra can be a very useful tool for the characterization of special nuclear material. A significant advantage in this method is the ability to convert a light-output PHD into the more meaningful neutron energy spectrum. This spectrum then allows key features of the sample to be observed (for example, the characteristic spontaneous fission and alpha-neutron peaks). This unfolding technique also has the capability of resolving other neutron samples, such as Pu–Be, Am–Li, Am–Be sources, as well as mono-energetic D–T and D–D sources. This technique is heavily dependent on the quality and size of the measured-PHD. With careful and accurate measurement techniques, it is possible to produce a reliable unfolded neutron energy spectrum that can be used for source identification.

References

[1] G.F. Knoll, in: Radiation Detection and Measurement, third ed., Wiley and Sons, 2003, pp. 220.
[2] J.L. Dolan, M. Flaska, S.A. Pozzi, D. Chichester., J. Nucl. Mater. Manage. 38 (1) (2009) 40.
[3] S.A. Pozzi, S.D. Clarke, M. Flaska, P. Peerani, Nucl. Instr. and Meth. in Phys. Res. A 608 (2009) 310.
[4] R. Koohi-Fayegh, Stuart Green, Malcolm C. Scott, Nucl. Instr. and Meth. A 460 (2001) 391.
[5] W.R. Burrus, FERD and FERDOR type unfolding codes, Report ORNL/RSIC-40, pp. 2–23, 1976.
[6] S. Avdic, S.A. Pozzi, V. Protopopescu, Nucl. Instr. and Meth. A 565 (2006) 742.
[7] Y. Xu, T. Downar, M. Flaska, A sequential least-squared algorithm for neutron spectrum unfolding from pulse-height distributions measured with liquid scintillators, (M&C+SNA), pp. 11, 2007.
[8] S.A Pozzi, E. Padovani, M. Marseguerra, Nucl. Instr. and Meth. in Phys. Res. A 513 (2003) 550.
[9] L. Cartegni, S.A. Pozzi, Measurement and simulation of liquid scintillator neutron response, ORNL TM-2004/315.
[10] S. Guardini, G. Guzzi, F. Mousty, S. Baumann, E. Kuhn, P. de Regge, PERLA: quality control provisions applied in the preparation and characterization of Pu-bearing Perla Standards. Report EUR 13308EN, CEC–JRC Ispra, 1990.
[11] E.F. Shores, Appl. Radiat. Isot. 62 (2005) 699.
[12] S.D. Clarke, M. Flaska, S.A. Pozzi, P. Peerani, Nucl. Instr. and Meth. A 604 (2009) 618.
[13] M. Flaska, S.A. Pozzi, Nucl. Instr. and Meth. A 577 (2007) 654.